

Precipitation in Fe- or Ni-implanted and annealed GaAs

J. C. P. Chang^{a)} and N. Otsuka^{b)}

School of Materials Engineering, Purdue University, West Lafayette, Indiana 47907

E. S. Harmon, M. R. Melloch, and J. M. Woodall

School of Electrical Engineering, Purdue University, West Lafayette, Indiana 47907

(Received 23 June 1994; accepted for publication 26 September 1994)

We report the formation of metal/semiconductor composites by ion implantation of Fe and Ni into GaAs and a subsequent anneal to nucleate clusters. Electron diffraction experiments and high resolution transmission electron microscopy images indicate that these precipitates are probably hexagonal and metallic Fe_3GaAs or Ni_3GaAs with orientation relationship to GaAs of $(10\bar{1}0)_{pp} \parallel (42\bar{2})_m$, $(0002)_{pp} \parallel (11\bar{1})_m$, and $[\bar{1}2\bar{1}0]_{pp} \parallel [011]_m$. Correlation of the electrical and structural properties of the samples annealed at different temperatures shows that the buried Schottky-barrier model has general applicability. © 1994 American Institute of Physics.

Metal-semiconductor composites, such as GaAs:As with small As precipitates dispersed in a GaAs matrix, have demonstrated remarkable electronic and optical properties. GaAs:As can suppress sidgating or backgating in GaAs integrated circuits by providing excellent device isolation.¹ In addition, this composite exhibits reasonable mobilities and in some cases subpicosecond lifetimes, which make it useful for ultrafast photoconductive switch applications.² GaAs:As has also demonstrated unusual optical properties.³ Although some controversy still remains, the optoelectronic properties can be explained by the depletion action of buried Schottky barriers associated with the As precipitates.⁴

Recent calculations⁵ show that metals can have stronger effects on the dielectric and optical properties of composites, thus making it attractive to search for a substitute to the semimetallic As precipitates in GaAs. A variety of experimental techniques, including molecular beam epitaxy (MBE) growth of GaAs at low temperatures⁶ and ion implantation,⁷ have been employed to fabricate GaAs:As. In this letter we introduce a technique to form composites using ion implantation of the transition metals Fe or Ni into GaAs and a subsequent anneal to nucleate clusters. Transition metals were chosen because they are important in semiconductor technology and they can easily form precipitates in semiconductors,⁸ e.g., Fe_2As microclusters in Fe grown on GaAs by MBE,⁹ and Fe-containing compounds in GaAs grown on FeGa films,¹⁰ or in Fe-doped GaAs grown by liquid encapsulation Czochralski.^{11,12} Here we present detailed transmission electron microscopy (TEM) studies and electrical measurements of the novel GaAs:Fe and GaAs:Ni composites.

GaAs samples were implanted with 1×10^{16} ions/cm² of Fe^+ or Ni^+ at an energy of 170 keV and at room temperature. TRIM simulations¹³ of final ion distributions indicate a range of 85 nm, a straggle of 45 nm, and a peak concentration of 9×10^{20} /cm³, i.e., ~ 4 at. % in GaAs. The latter is well

above the Fe solubility limit in GaAs at 950 °C $\sim 3 \times 10^{17}$ /cm³. The samples were further annealed in a rapid thermal processor at 950 °C for 30 s or at 600 °C for 30 min with GaAs proximity caps. The (011) cross-sectional transmission electron microscopy (XTEM) specimens were prepared by standard ion milling and then observed with a Jeol 2000 EX electron microscope. Scanning electron microscopy (SEM) examination was performed on a Jeol JSM-35CF.

The (004) x-ray rocking curve of the as-implanted samples had an extra peak observed towards smaller angles, indicating an expansion in the lattice in the implanted region. After annealing only a sharp substrate peak with FWHM of 14 arcsec was seen. This suggests that most of the strain in the GaAs matrix was relaxed by precipitation, which was also verified by TEM. TEM analysis of the annealed material revealed a composite structure consisting of metal clusters in a GaAs matrix. Figure 1 is a bright-field XTEM image for the Fe-implanted sample that was annealed at 950 °C for 30 s. End-of-range damage in the form of dislocation loops (marked "dl") is present at a depth of 170–600 nm below the surface. From the surface to a depth of about 170 nm, precipitates of different sizes are found to be surrounded by a GaAs crystal. The size of a typical precipitate (marked "p") is 35 nm in diameter with moiré fringes clearly seen. The

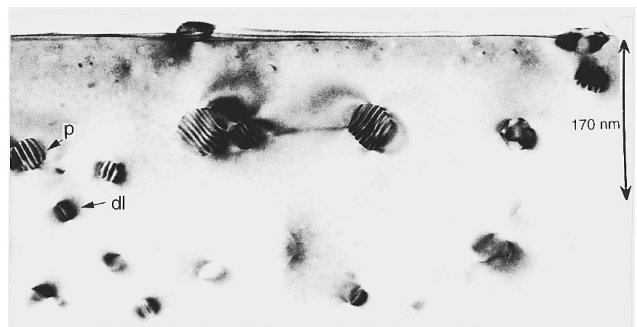


FIG. 1. Bright-field TEM image of a GaAs region that was implanted with Fe and annealed for 30 s at 950 °C. Precipitates (p) highlighted with moiré fringes and dislocation loops (dl) are observed at different depths below the surface. Similar results hold for the Ni-implanted GaAs.

^{a)}Present address: School of Electrical Engineering, Purdue University, West Lafayette, IN 47907.

^{b)}Present address: Department of Materials Science, Japan Advanced Institute of Science and Technology, Hokuriku, Nomigun, Ishikawa 923-12, Japan.

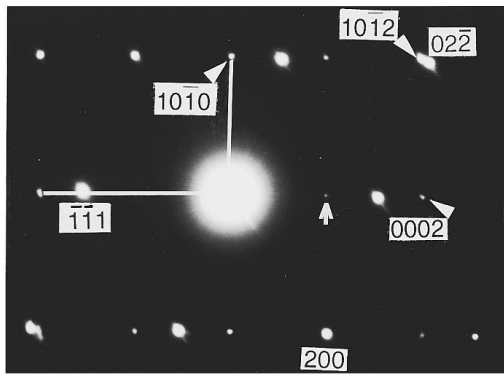


FIG. 2. Typical SADP of a precipitate in the Fe-implanted GaAs sample that was annealed at 950 for 30 s. The electron beam is along a $\langle 011 \rangle$ direction of GaAs. Weak spots marked by arrows are from the precipitate.

separation between the precipitates is about 100 nm. However, precipitates within about 40 nm of the surface are smaller (6 nm in diameter) with larger (90 nm) precipitates protruding from the surface. The precipitates are not all spherical. Some of them appear faceted along the $\{111\}$ GaAs planes as their size gets larger. The facet formation will be discussed at the end of the next paragraph. SEM images showed about $10^9/\text{cm}^2$ of large precipitates (90 nm) lying on the surface, consistent with the TEM observation.

In an effort to determine the phase and structure of these precipitates, selected area diffraction patterns (SADPs) were analyzed from three different zone axes of GaAs obtained by specimen tilting. In the SADP, weak spots appear in addition to the spots of GaAs. One example is shown in Fig. 2 for the Fe-implanted sample along a $\langle 011 \rangle$ pole. A dark-field image taken by using one of these weak spots showed that the precipitates in the regrown layer appeared with bright contrast. This observation suggests that the precipitates have a different crystal structure from that of GaAs and have a particular orientation relationship with respect to the surrounding GaAs crystal. The spot spacings and angles with respect to the transmitted beam were compared to those calculated for 10 candidate crystals: α -Fe, ϵ -Fe, γ -Fe, FeAs, FeAs₂, Fe₂As, Fe₃Ga₄, Fe₃Ga, FeGa₃, and Fe₃GaAs. Of these only FeAs and Fe₃GaAs can explain any of the diffraction patterns. The orthorhombic FeAs can fit the patterns along the $\langle 233 \rangle$ and $\langle 012 \rangle$ poles but not the $\langle 011 \rangle$ one due to forbidden diffraction of its (001) plane. Good matches to all three patterns were only found with the hexagonal ternary compound Fe₃GaAs ($a=0.402$, and $c=0.503$ nm).^{11,12} Thus, weak spots indicated by arrows in Fig. 2 correspond to the $(10\bar{1}0)$ and (0002) planes of Fe₃GaAs. The orientation relationship is given by $(10\bar{1}0)\text{Fe}_3\text{GaAs} \parallel (42\bar{2})\text{GaAs}$, $(0002)\text{Fe}_3\text{GaAs} \parallel (11\bar{1})\text{GaAs}$, and $[1\bar{2}10]\text{Fe}_3\text{GaAs} \parallel [011]\text{GaAs}$. This orientation relationship is normally reported for a hexagonal precipitate embedded in a cubic matrix and is believed to provide the lowest strain energy obtainable by the precipitates within this matrix given the excellent match (mismatch=0.5%) between the $(10\bar{1}0)\text{Fe}_3\text{GaAs}$ ($d=0.3481$ nm) and the projection of $(002)\text{GaAs}$ on $(111)\text{GaAs}$ ($d=0.3462$ nm).

One interesting feature to be noticed in Fig. 2 is the occurrence of extra spots at $1/2(0002)$ positions, which are

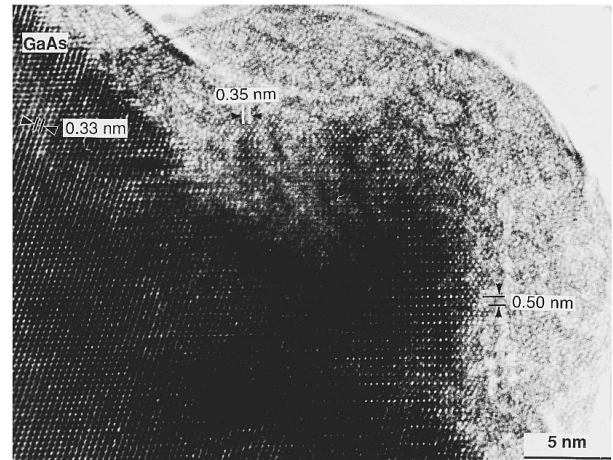


FIG. 3. $[011]$ HRTEM image of the Fe-implanted GaAs that was annealed at 950 °C for 30 s showing a precipitate in a GaAs matrix.

forbidden diffractions of Fe₃GaAs. This occurrence can be generally attributed to double diffraction from $(11\bar{1})\text{GaAs}$ and $(10\bar{1}0)\text{Fe}_3\text{GaAs}$ or ordering of Fe₃GaAs along the $[0002]$ direction. The latter is more likely as shown by high resolution TEM (HRTEM) images. Figure 3 is $\langle 011 \rangle$ HRTEM image of the precipitate (marked p in Fig. 1) after rethinning with part of the GaAs matrix milled away. Regions without severe damage clearly show orthogonal lattice fringes with spacings of 0.35 and 0.50 nm, corresponding to the $(10\bar{1}0)$ and (0001) planes of Fe₃GaAs, respectively. The (0002) lattice images appear weaker than the (0001) superstructure lattice images. The doubling of the (0002) fringes as well as the superspots in the diffraction pattern indicate the occurrence of ordering in the precipitate. To our knowledge no ordering has been reported with FeAs. The Fe₃Ga_{2-x}As_x alloys, which can exist over a range of composition, undergo a change in structure to more ordered variants with increasing gallium content at $x \approx 0.85$.¹² This change is consistent with ordering of vacancies in the Fe sites. Another difference between these two candidate crystals is that FeAs is antiferromagnetic and Fe₃GaAs is ferromagnetic. Magnetic measurements may offer clues to the phase identification.

As in the case for GaAs:As,¹⁴ the average size and corresponding density of the Fe₃GaAs precipitates can be controlled by the temperature and duration of the anneal. Figure 4 is a $[011]$ HRTEM image showing the 140 ± 20 nm regrown layer of the Fe-implanted sample that was annealed at 600 °C for 30 min. Small round-shaped precipitates (3–5 nm in diameter) are seen homogeneously distributed in GaAs from the depth of 40 nm throughout the entire regrown layer. The average separation between these precipitates is about 3 nm. From the surface to the depth of 40 nm, larger precipitates (6–7 nm) highlighted with moiré fringes appear to accumulate underneath the surface without protruding the surface as seen in the sample annealed at 950 °C. These observations agree with the reported Fe outdiffusion in other Fe-implanted GaAs using secondary-ion-mass spectroscopy.¹⁵

The Ni samples look very similar to the Fe samples under both the image and diffraction modes of TEM. It is rea-

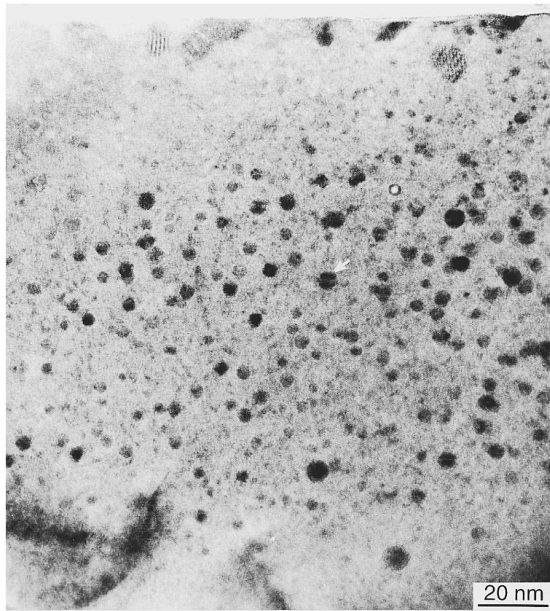


FIG. 4. [011] HRTEM image of the Fe-implanted GaAs that was annealed at 600 °C for 30 min showing the presence of precipitates (arrowed) within the GaAs matrix. Similar results hold for the Ni-implanted GaAs.

sonable to assume that the precipitates in these two samples have the same structure. Unlike FeAs, NiAs is hexagonal and it cannot explain the diffraction pattern. The diffraction pattern was therefore identified as being due to a hexagonal Ni_3GaAs ¹⁶ ($a=0.39$, and $c=0.501$ nm) with an orientation relationship given by $(10\bar{1}0)\text{Ni}_3\text{GaAs}\parallel(42\bar{2})\text{GaAs}$, $(0002)\text{Ni}_3\text{GaAs}\parallel(11\bar{1})\text{GaAs}$, and $[\bar{1}2\bar{1}0]\text{Ni}_3\text{GaAs}\parallel[110]\text{GaAs}$. Sands *et al.*¹⁶ reported Ni_3GaAs resulting from the interaction of deposited Ni thin films and GaAs and proposed a structure for Ni_3GaAs , which is very similar to the aforementioned Fe_3GaAs structure. One difference between their work and our results is that we did not observe decomposition of Ni_3GaAs at high temperatures (>400 °C) as they did. This may be due to different experimental conditions.

Hall effect measurements on the Fe and Ni samples annealed at 950 °C for 30 s showed that they are both p type with carrier concentrations of 2.5 and $7.5 \times 10^{17}/\text{cm}^3$ (assuming the carriers are confined to the 170-nm-thick regrown layer), and mobilities of 179 and 252 $\text{cm}^2/\text{V s}$, respectively. The carrier concentration and mobility could not be determined for the samples annealed at 600 °C for 30 min because they are highly resistive and the Hall measurement is dominated by conduction through the semi-insulating GaAs substrate. The electrical properties correlate with the structural properties showing that Fe_3GaAs or Ni_3GaAs precipitates appear to act as buried Schottky barriers,⁴ depleting carriers from the GaAs region around the precipitates. In this con-

nection, the layer becomes semi-insulating when the precipitate density is high enough for the depletion regions surrounding the precipitates to overlap, which has been observed in $\text{GaAs}:\text{As}$ ⁴ and $\text{InP}:\text{In}_x\text{Cu}$.¹⁷

In conclusion, we report the formation of metal/semiconductor composites by ion implantation of the transition metals Fe and Ni into GaAs and a subsequent anneal to nucleate clusters. Electron diffraction experiments and HRTEM images identified these precipitates as hexagonal, metallic Fe_3GaAs , or Ni_3GaAs with the orientation relationship with respect to GaAs by $(10\bar{1}0)_{pp}\parallel(42\bar{2})_m$, $(0002)_{pp}\parallel(11\bar{1})_m$, and $[\bar{1}2\bar{1}0]_{pp}\parallel[110]_m$. Nearly perfect lattice match between the $(10\bar{1}0)_{pp}$ and the projection of $(002)_m$ on $(11\bar{1})_m$ leads to the formation of facet along $(11\bar{1})_m$. The doubling of the (0002) fringes as well as the superspots in the diffraction pattern indicates the occurrence of ordering in the precipitate. The sizes and densities of the precipitates can be controlled by the annealing temperatures. Correlation of the electrical and structural properties of the samples at different temperatures indicate that the buried Schottky-barrier model has general applicability. The ability to form these composites with different metals may allow an additional degree of control of the composite properties.

This work was partially supported by the US Air Force Office of Scientific Research under Grant Nos. F49620-93-1-0031 and F49620-93-1-0388.

- ¹F. W. Smith, A. R. Calawa, Chang-Lee Chen, M. J. Mantra, and L. J. Mahoney, IEEE Electron Device Lett. **EDL-9**, 77 (1988).
- ²A. C. Warren, N. Katzenellenbogen, D. Grischkowsky, J. M. Woodall, M. R. Melloch, and N. Otsuka, Appl. Phys. Lett. **58**, 1512 (1991).
- ³D. D. Nolte, M. R. Melloch, J. M. Woodall, and S. E. Ralph, Appl. Phys. Lett. **62**, 1356 (1993).
- ⁴A. C. Warren, J. M. Woodall, J. L. Freeouf, D. Grischkowsky, D. T. McInturff, M. R. Melloch, and N. Otsuka, Appl. Phys. Lett. **57**, 1331 (1990).
- ⁵D. D. Nolte, J. Appl. Phys. **76**, 3740 (1994).
- ⁶M. R. Melloch, N. Otsuka, J. M. Woodall, A. C. Warren, and J. L. Freeouf, Appl. Phys. Lett. **57**, 1531 (1990).
- ⁷A. Claverie, F. Namavar, and Z. Liliental-Weber, Appl. Phys. Lett. **62**, 1271 (1993).
- ⁸E. R. Weber, Appl. Phys. A **30**, 1 (1983).
- ⁹J. J. Krebs, B. J. Jonker, and G. A. Prinz, J. Appl. Phys. **61**, 2596 (1987).
- ¹⁰F. Wang, K. M. Chen, and P. I. Cohen, the 1993 Electronic Materials Conference, Santa Barbara, CA, 23–25 June 1993 (unpublished).
- ¹¹I. R. Harris, N. A. Smith, B. Cockayne, and W. R. MacEwan, J. Cryst. Growth **82**, 450 (1987).
- ¹²C. Greaves, E. J. Devlin, N. A. Smith, I. R. Harris, B. Cockayne, and W. R. MacEwan, J. Less-Common Metals **157**, 315 (1990).
- ¹³J. F. Ziegler, J. P. Biersack, and U. Littmark, *The Stopping and Range of Ions in Solids* (Pergamon, New York, 1985), Vol. 1.
- ¹⁴M. R. Melloch, J. M. Woodall, N. Otsuka, K. Mahalingam, C. L. Chang, D. D. Nolte, and G. D. Pettit, Mater. Sci. Eng. B **22**, 31 (1993).
- ¹⁵H. Ullrich, A. Knecht, D. Bimberg, H. Käutle, and W. Schlaak, J. Appl. Phys. **72**, 3514 (1992).
- ¹⁶T. Sands, V. G. Keramidis, J. Washburn, and R. Gronsky, Appl. Phys. Lett. **48**, 402 (1986).
- ¹⁷R. P. Leon, M. Kaminska, K. M. Yu, and E. R. Weber, Phys. Rev. B **46**, 12460 (1992).